

# High-throughput prediction of thermodynamically stable 1D magnetic transition-metal chalcogenides and halides

Canbo Zong<sup>1,2,#</sup>, Deping Guo<sup>3,#</sup>, Renhong Wang<sup>1,2</sup>, Weihang Zhang<sup>1,2</sup>, Jiaqi Dai<sup>1,2</sup>, Zhongqin Zhang<sup>1,2</sup>, Cong Wang<sup>1,2,\*</sup>, Xianghua Kong<sup>4</sup>, and Wei Ji<sup>1,2,\*</sup>

<sup>1</sup>*Beijing Key Laboratory of Optoelectronic Functional Materials & Micro-Nano Devices, School of Physics, Renmin University of China, Beijing 100872, China*

<sup>2</sup>*Key Laboratory of Quantum State Construction and Manipulation (Ministry of Education), Renmin University of China, Beijing, 100872, China*

<sup>3</sup>*College of Physics and Electronic Engineering, Center for Computational Sciences, Sichuan Normal University, Chengdu, 610101, China*

<sup>4</sup>*College of Physics and Optoelectronic Engineering, Shenzhen University, Shenzhen 518060, China.*

\*Corresponding authors. Email: [wcphys@ruc.edu.cn](mailto:wcphys@ruc.edu.cn)(C.W.) [wji@ruc.edu.cn](mailto:wji@ruc.edu.cn) (W.J.).

**Abstract:** The search for novel one-dimensional (1D) materials with exotic physical properties is crucial for advancing nanoelectronics and spintronics[1]. Here, we perform a comprehensive high-throughput, first-principles study to explore the vast landscape of 1D transition-metal chalcogenides and halides[2]. Starting with 6,832 candidate structures derived from 28 metals and 8 non-metals, we systematically evaluated their thermodynamic stability by comparing the formation energies of 1D chains against competing 2D phases, mimicking thermodynamic selectivity during nucleation. This screening identified 210 stable 1D magnetic chains. Furthermore, representation learning models revealed that chemical stoichiometry and the electron affinity of the non-metal element are key factors governing 1D stability. The stable materials exhibit a rich spectrum of properties, including diverse magnetic orders (FM, AFM) and Luttinger compensated antiferromagnetism in MnTe[3]. We discovered 20 ferroelastic chains, with FeTe showing a giant magnetostriction of -5.57%[4]. Other emergent phenomena include Charge Density Wave (CDW) chains in FeTe and NiSe[5]. Finally, our findings propose concrete platforms for quantum applications, such as the predicted realization of Majorana zero modes in a ferromagnetic CrCl<sub>2</sub> chain on a superconducting NbSe<sub>2</sub> substrate[6].

## Introduction

Two-dimensional (2D) van der Waals (vdW) layers have garnered increasing attentions in the past two decades, yielding a growing family with diverse physical properties[7], such as magnetism[8], charge density waves (CDWs)[9], and strong correlation effects. Although interlayer interactions in 2D materials are typically considered non-covalent, many properties exhibit strong layer-number dependence due to electronic hybridization of out-of-plane states between layers, known as covalent-like quasi-bonding[10]. In one-dimensional (1D) vdW chains, such coupling occurs in two transverse directions, leading to enhanced geometric and electronic anisotropy, stronger chain-number dependence, and thus more fruitful inter-chain stacking flexibility and tunability. Moreover, the 1D geometric characteristic intrinsically reduces coordination numbers of atoms, which amplifies thermal and quantum fluctuation effects[11] and highlights effects arising from interfacial contacts. Furthermore, strong quantum confinements in 1D substantially suppress the kinetic energy, leading to largely enhanced electronic correlations. Importantly, the reduced dimensionality of 1D systems also renders them more tractable for theoretical modeling, enabling more direct comparisons between experimental observations and exact or near-exact models. As such, 1D vdW materials provide a compelling platform for exploring correlated quantum phases, such as Luttinger liquid, Mott insulating states, and magnetic orders, bridging long-standing gaps between condensed matter theory and experiments[12].

Magnetism is the most historical, widespread, and readily observed correlated phenomenon in solids[13]. Although some magnetic chains were theoretically predicated[14], the experimental realization of 1D vdW chains was found exceptionally challenging. For a given composition, the 1D and 2D structures compete with each other, and the 2D counterpart usually has better thermal stability, obscuring the presence of 1D chains[15]. A straightforward strategy for the experimental preparation of 1D magnetic chains lies in preventing the presence of 2D flakes in a spatially confined space. Carbon nanotubes were used to construct these confined spaces, in which  $\text{CrX}_3$  and  $\text{CrX}_2$  ( $\text{X}=\text{Cl}/\text{Br}/\text{I}$ ), and  $\text{VTe}_n$  ( $n=1,2,3$ ) single-atomic chains were very recently

synthesized[16][17]. For free-standing vdW magnetic chains, the first demonstration was achieved very recently in  $\text{CrCl}_3$  chains, in which a tunable chemical potential strategy was employed to stabilize the 1D structure at the initial growing stage[15]. In the  $\text{CrCl}_3$  case, the 1D vdW chain exhibits a free energy lower than that of an edge unit of its 2D monolayer counterpart, highlighting the importance of comparing 1D and 2D free energies across the entire chemical potential range in theoretical predictions[15].

However, none previous prediction ever considered free-energy. Even without consideration of free-energy, a high-throughput calculation on likely 1D magnetic chains is surprisingly missing. Here, we performed a high-throughput DFT survey of >6 000 candidate 1D transition-metal chalcogenide and halide chains. Thermodynamic ranking against competing 2D polymorphs yielded 210 stable magnetic chains. Machine-learning analysis shows that stoichiometry and anion electron affinity chiefly govern stability. The resulting set features diverse FM and AFM orders including a Luttinger-compensated AFM MnTe chain, 20 strongly magnetoelastic chains (e.g., FeTe,  $-5.6\%$  magnetostriction), several CDW systems, and a  $\text{CrCl}_2$  chain on  $\text{NbSe}_2$  predicted to host Majorana zero modes, offering concrete platforms for quantum-device applications.

## Results and discussion

Our high-throughput computational workflow, detailed in Figure 1, was designed to systematically explore the vast chemical space of 1D transition-metal chalcogenides and halides. In the initial step, a combinatorial library of 6,832 candidate structures was generated. To assess their viability, we performed a rigorous thermodynamic stability analysis. The formation energy of each 1D chain was calculated across a range of non-metal chemical potentials and benchmarked against the formation energies of competing 2D polymorphs (with 1:2 and 1:3 stoichiometries) and elemental bulk phases. A 1D chain was deemed thermodynamically stable only if it represented the ground state within a specific interval of the chemical potential. This critical step, which mimics the thermodynamic selectivity that governs experimental synthesis during nucleation, allowed us to filter the vast initial pool down to 210 unique,

thermodynamically stable 1D chains. The magnetic ground states of these stable chains were diverse, comprising 40 ferromagnetic (FM), 43 AB-type antiferromagnetic (AFM), 25 AABBB-type AFM, 4 AFM-Half, and 98 non-magnetic (NM) materials (see Fig. 1(b)).

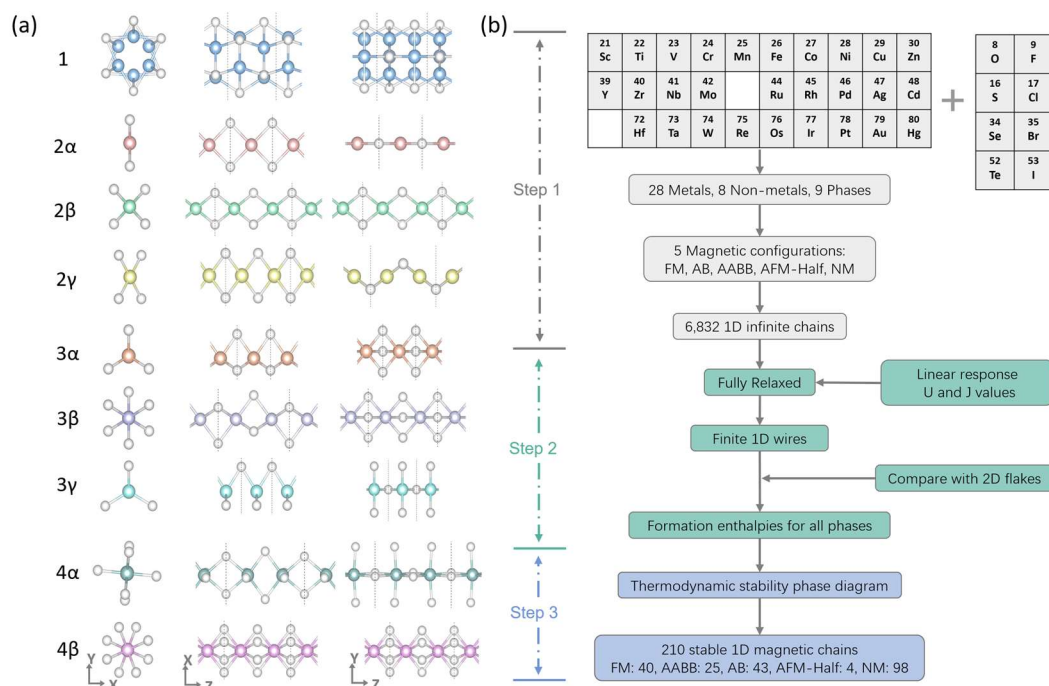
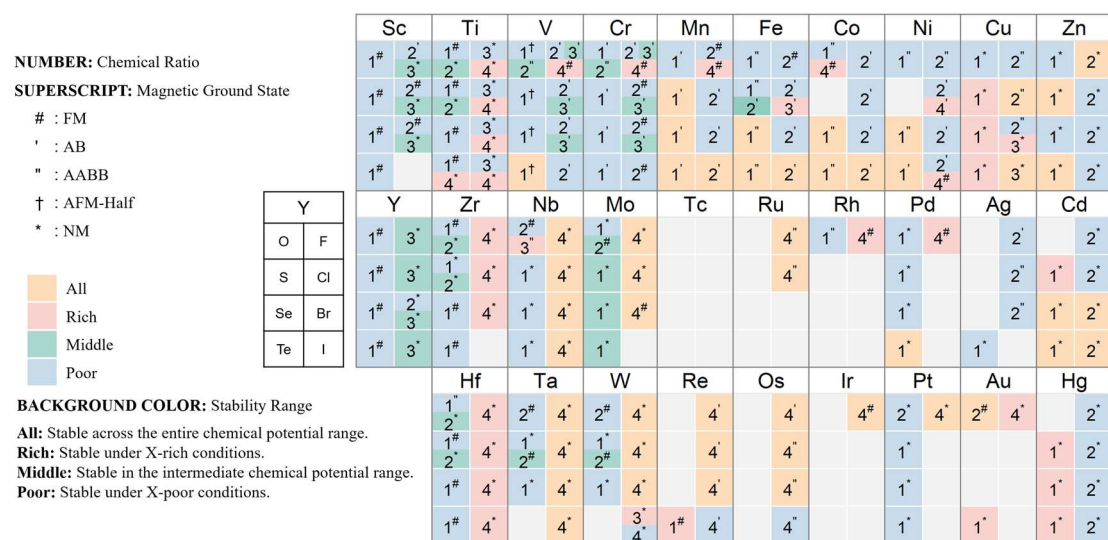


**Fig. 1. High-throughput computational workflow for the discovery of stable 1D magnetic materials.** (a) Nine distinct structural polymorphs of 1D chains considered in the screening process. Each row displays the top view (left), perspective view (middle), and side view (right) for a given phase, which are labeled from 1 to 4 $\beta$ . The coordinate axes are shown in the bottom left. (b) A schematic of the three-step computational screening methodology. Step 1 outlines the high-throughput generation of 6,832 unique infinite 1D chains from a library of elements and phases, followed by structural relaxation. Step 2 describes the thermodynamic stability analysis, where formation enthalpies are computed to construct a stability phase diagram. Step 3 illustrates the final filtering process, resulting in 210 predicted stable 1D magnetic chains, with a summary of their magnetic ground states.

To visualize the landscape of these stable materials, we consolidated our findings into a comprehensive periodic table-style plot, as shown in Figure 2. This plot serves as a roadmap, detailing the stable stoichiometries, magnetic ground states, and stability windows for combinations of 28 transition metals and 8 non-metals. Several clear and chemically intuitive trends emerge from this map.

First, a strong periodic trend is evident. The 4th-period transition metals (Sc to Zn) are the most prolific in forming stable 1D chains, and they host the vast majority of the magnetic materials discovered. This suggests that the localized nature of 3d orbitals is particularly conducive to forming stable, low-dimensional magnetic structures. In contrast, while the 5th and 6th-period transition metals also form a considerable number of stable chains, a larger fraction of them are non-magnetic. This trend is exemplified by the Group 12 elements (Zn, Cd, Hg), whose chains are exclusively non-magnetic due to their completely filled d-shells, which preclude the formation of local magnetic moments.



chains. This suggests that the high electronegativity and small ionic radii of early halogens are highly effective at stabilizing the 1D morphology, likely through the formation of strong, highly ionic bonds. As one moves down the halogen or chalcogen groups (e.g., from F to I, or O to Te), the number of stable chains generally decreases, indicating that larger, less electronegative anions are less effective at stabilizing these low-dimensional structures.

Third, the material's stoichiometry is intimately linked to the chemical potential of the synthesis environment. As shown in Figure 2, 1:1 (MX) chains tend to be stable under non-metal-poor conditions, where there is a relative scarcity of anion atoms. Conversely, 1:4 (MX<sub>4</sub>) chains are predominantly stable under non-metal-rich conditions, where an abundance of anions favors structures with higher metal coordination. This intuitive result provides a direct recipe for experimental synthesis: tuning the partial pressure or concentration of the non-metal precursor can selectively target different 1D stoichiometries. Furthermore, we identified several materials, primarily with 1:1 and 1:4 stoichiometries, that are stable across the entire range of the non-metal chemical potential (indicated by the 'All' stability range). These materials, such as TiI<sub>4</sub>, ZrI<sub>4</sub>, and MoCl<sub>4</sub>, are exceptionally robust and should be the most readily synthesizable in freestanding form.

To move beyond qualitative trends and identify the fundamental electronic and structural descriptors governing stability, we employed a machine learning (ML) approach. This investigation was motivated by the question: what makes a 1D chain thermodynamically stable? Using the results of our high-throughput screening as a training dataset, we developed a Random Forest classification model to predict whether a given chain is stable. The initial features included elemental properties such as atomic number, density, atomic radius, electron affinity (EA), ionization energy (IE), and Pauling electronegativity (PE), alongside the chemical ratio (stoichiometry).

The feature importance analysis, shown in Figure 3(a), reveals a clear hierarchy of factors. The single most important feature, with an importance score exceeding 35%, is the chemical ratio (Ratio). This is physically intuitive, as stoichiometry dictates the fundamental crystal structure, coordination environment, and bond saturation, which

are the primary determinants of cohesive energy. Following stoichiometry, the next most important features are properties of the metal atom ( $_1$ ), including its density (Dens $_1$ ), atomic number (AN $_1$ ), and atomic radius (ratom $_1$ ). These features are all strongly correlated and collectively represent the size and core electronic structure of the cation. For the non-metal anion ( $_2$ ), electron affinity (EA $_2$ ) emerges as the most critical descriptor. This highlights the crucial role of the anion's ability to accept charge from the metal, indicating that the degree of ionic bonding is a key stabilizing force.

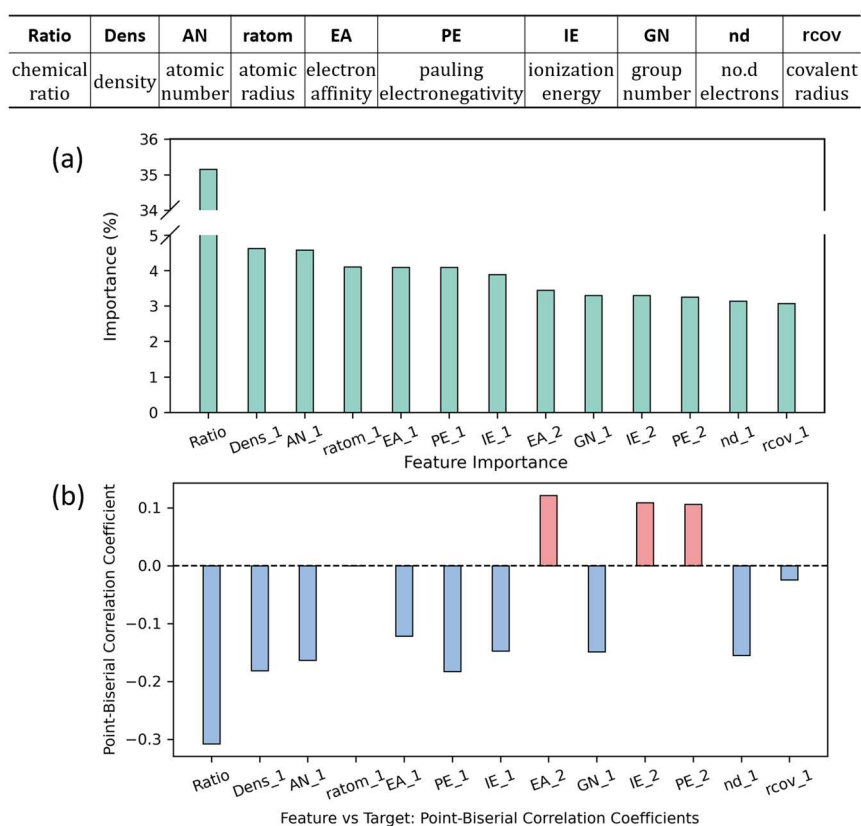


**Fig. 3. Feature importance and correlation analysis for the machine learning model of 1D material stability.** A legend at the top defines the abbreviations for the elemental properties used as features. (a) Relative feature importance in the trained classification model. The bar chart indicates the percentage importance of each descriptor, with the chemical ratio (Ratio) identified as the most significant predictor. (b) Point-biserial correlation coefficients between the input features and the material stability target. The bars represent the nature of the correlation, where blue bars indicate a negative correlation (a higher feature value corresponds to instability) and red bars indicate a positive correlation.

To understand the directionality of these influences, we performed a point-biserial correlation analysis between the top features and the stability target, with results shown in Figure 3(b). We found a strong negative correlation between stability and both the Ratio and the metal's atomic number (AN\_1). The negative correlation with Ratio confirms that higher-stoichiometry chains (e.g., 1:4 vs. 1:1) are generally less likely to be stable across the entire dataset. The negative correlation with AN\_1 quantitatively confirms the trend observed in Fig. 2: heavier transition metals from the 5th and 6th periods are less likely to form stable 1D chains than their 4th-period counterparts. Conversely, we observe a strong positive correlation between stability and the non-metal's electron affinity (EA\_2), ionization energy (IE\_2), and electronegativity (PE\_2). All three features point to the same physical principle: a non-metal that strongly attracts and binds electrons is far more likely to form a stable 1D chain. This ML result perfectly explains the universal stability of fluoride chains seen in Fig. 2, as fluorine possesses the highest electron affinity and electronegativity of all elements. These ML-derived insights provide powerful, quantitative design rules for the experimental discovery of new 1D materials.

The 210 stable chains provide a rich playground for discovering exotic quantum phenomena. Our detailed analysis revealed several compelling systems, highlighted in Figure 4.

Among the chains with an AABB magnetic configuration, we identified FeTe and NiSe as intrinsic CDW systems (Fig. 4(a, b)). In their primitive 1x2 unit cells, both chains are metallic. However, upon expanding to a 1x4 supercell, they spontaneously undergo a Peierls transition. This electronic instability, characteristic of 1D metals, is driven by Fermi surface nesting, which allows the system to lower its total energy by opening a band gap at the Fermi level. This electronic transition is coupled to a periodic lattice distortion, resulting in the 1x4 structural periodicity. Notably, this CDW formation coexists with the underlying AABB magnetic order, indicating a complex interplay between the charge, lattice, and spin degrees of freedom in these materials.



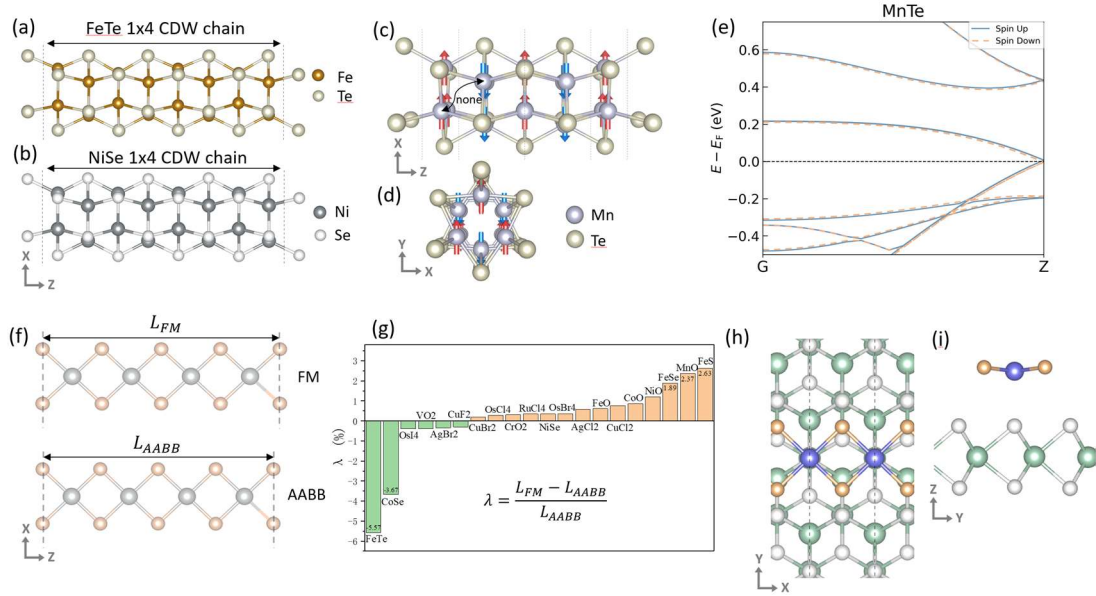


**Fig. 4. Atomic structures, electronic properties, and magnetostriction of exemplary 1D van der Waals magnetic materials.** (a, b) Atomic structures of FeTe and NiSe chains, which form 1x4 Charge Density Wave (CDW) superstructures. (c, d) Side and top views of the atomic and magnetic structure of a 1D MnTe chain. The red and blue arrows on the Mn atoms denote the spin orientation, characteristic of a Luttinger compensated antiferromagnet. (e) The calculated electronic band structure for the MnTe chain, with spin-up and spin-down channels shown. (f) A schematic illustrating magnetostriction by comparing the lattice parameter of a ferromagnetic (FM) chain to that of an AABF-type antiferromagnetic chain. (g) A chart of calculated magnetostriction coefficients ( $\lambda$ ) for various 1D materials. (h, i) An illustration of a heterostructure, showing the top view of a ferromagnetic CrCl2 chain on a NbSe2 bilayer and isolated views of the CrCl2 chain.

In our survey of AB-type antiferromagnets, MnTe emerged as a particularly unusual case (Fig. 4(c, d)). Its calculated band structure (Fig. 4(e)) displays a distinct energy splitting between spin-up and spin-down bands, even though the net magnetization is zero, a feature not found in conventional collinear antiferromagnets. A detailed symmetry analysis revealed that the MnTe chain possesses a reduced structural symmetry compared to other 1:1 chains, with the key feature being the absence of any symmetry operation (like inversion or a two-fold rotation) that connects the two spin-polarized Mn sublattices. This broken symmetry lifts the spin degeneracy of the energy bands, leading to a state known as Luttinger-compensated

antiferromagnetism. This property makes MnTe a promising material for spintronic applications that exploit spin-polarized currents without generating stray magnetic fields.

Given their structural softness, 1D chains are expected to exhibit strong coupling between lattice and spin degrees of freedom. We quantified this by calculating the magnetostriction coefficient ( $\lambda$ ), defined as the percentage change in lattice constant when switching the magnetic ground state from AABB to FM (Fig. 4(f)). As shown in Figure 4(g), we discovered giant magnetostriction in several 1D chains. The FeTe chain exhibits a colossal  $\lambda$  of -5.57%, while CoSe shows a value of -3.67%. These values are more than an order of magnitude larger than that of the archetypal magnetostrictive material Terfenol-D ( $\sim 0.2\%$ ). This exceptionally large response signifies a massive change in physical dimensions driven by a change in magnetic order, identifying these AABB chains as ferroelastic. In a ferroelastic material, there are multiple stable lattice distortion states (here, associated with different magnetic orders) that can be switched by an external field (here, a magnetic field). These 1D chains represent a new class of nanoscale ferroelastic materials with potential applications in ultra-sensitive magnetic sensors and actuators.

Finally, we explored the potential of these 1D magnetic chains for topological quantum computing. A leading proposal for realizing Majorana zero modes involves creating a heterostructure of a ferromagnet and an s-wave superconductor. We identified the ferromagnetic CrCl<sub>2</sub> chain on a superconducting NbSe<sub>2</sub> substrate as an ideal candidate. Our calculations show that a freestanding CrCl<sub>2</sub> chain is thermodynamically stable under Cl-poor conditions and is ferromagnetic. As shown in Figure 4(h, i), when this chain is placed on a NbSe<sub>2</sub> monolayer, the most stable configuration involves the Cr atoms adsorbing on the Se-top sites. Crucially, the chain remains robustly ferromagnetic in this heterostructure, with a large local magnetic moment of 3.7  $\mu_B$  per Cr atom. This prediction provides a concrete, experimentally feasible vdW platform for realizing topological superconductivity and braiding Majorana modes, paving the way for fault-tolerant quantum computers.

## Conclusion

In conclusion, we have performed a comprehensive high-throughput, first-principles investigation to systematically explore the stability and properties of 1D transition-metal chalcogenides and halides. By developing a rigorous screening protocol that benchmarks the thermodynamic stability of 1D chains against competing 2D phases, we have successfully identified 210 unique, thermodynamically stable 1D magnetic chains from an initial pool of over 6,800 candidates. This work establishes the largest validated database of such materials to date, providing a crucial and expansive resource for future theoretical and experimental exploration.

Beyond the creation of this materials library, our study provides fundamental insights into the governing principles of 1D stability. The analysis, visualized in a comprehensive periodic-table map, reveals clear design rules related to elemental periodicity and anion chemistry, while our machine learning models quantitatively confirmed that chemical stoichiometry and the electron affinity of the non-metal anion are the two most dominant factors. These findings offer powerful, predictive capabilities for the targeted synthesis of new one-dimensional materials.

The rich portfolio of stable materials discovered hosts a remarkable spectrum of emergent quantum phenomena. We identified the coexistence of Charge Density Waves and AABB antiferromagnetism in FeTe and NiSe, uncovered Luttinger-compensated antiferromagnetism in MnTe, and, perhaps most strikingly, discovered a new class of 1D ferroelastic chains. These chains, such as FeTe, exhibit colossal magnetostriction coefficients (e.g., -5.57%) that are orders of magnitude larger than conventional materials, signifying an exceptionally strong spin-lattice coupling.

Ultimately, this work serves as both a comprehensive atlas and a predictive guide for the experimental community. The materials identified—from the ferroelastic chains suitable for nanoscale sensors and actuators to the promising CrCl<sub>2</sub>/NbSe<sub>2</sub> heterostructure for hosting Majorana zero modes in topological quantum computers—offer concrete and validated platforms to bridge the gap between theoretical prediction and experimental realization. We anticipate that our findings will significantly accelerate the discovery and application of novel 1D quantum materials in next-

generation electronics and quantum technologies.

## Methods

Calculations were performed using the generalized gradient approximation (GGA) in the Perdew-Burke-Ernzerhof (PBE) form for the exchange-correlation potential[18], the projector augmented wave (PAW) method[19], and a plane-wave basis set as implemented in the Vienna ab-initio simulation package (VASP)[20][21]. Grimme's semi-empirical D3 scheme for dispersion corrections (DFT-D3) was adopted to describe van der Waals (vdW) interactions[22]. To investigate the favored magnetic configurations of the freestanding 1D chains, supercells of  $1\times 1\times 2$  or  $1\times 1\times 4$  were employed, depending on the periodicity of the specific magnetic ordering. All structures were fully relaxed until the residual force per atom was less than  $0.01\text{ eV/\AA}$ . To account for on-site Coulomb interactions, the DFT+U method was applied to the 3d orbitals of V, Cr, Mn, Fe, Co, and Ni[23]. The effective Hubbard U and exchange J parameters for each compound were determined individually using a linear response method[24]. A vacuum layer of more than  $15\text{ \AA}$  was employed in all supercells to prevent interactions between adjacent chains in neighboring cells. An energy cut-off of  $700\text{ eV}$  was used for the plane wave basis set in all calculations involving the freestanding chains, and a uniform k-point grid of density  $9.6/\text{\AA}^{-1}$  was used to sample the first Brillouin zones. To determine the magnetic ground state, we considered several magnetic configurations, the scope of which depended on the stoichiometry. Specifically, for 1:1 chains, we investigated FM, NM, and three AFM states (ABAB, AABB, and AFM-Half). For other stoichiometries, the set was limited to FM, NM, ABAB, and AABB configurations. All structures were fully relaxed for each considered magnetic state. Formation enthalpies (H) for finite single chains and 2D flakes were calculated following the formula used in a previous publication[15].

Now, we introduce the high-throughput workflow used in this work. There are three steps in the workflow, as shown in Fig. 1. These three steps are represented by grey, green and blue sections, respectively. In the first step, we constructed a comprehensive initial database of one-dimensional (1D) chains. This was achieved by

systematically combining 28 transition metals with 8 non-metal elements across 9 different structural polymorphs (as shown in Fig. 1a). For each of these structural combinations, a set of competing magnetic orderings was evaluated to create our initial pool of candidates. This combinatorial approach resulted in a total of 6,832 unique, infinite 1D chains as candidates for further study. In the second step, we performed detailed calculations to determine the energetic properties of these candidates. We conducted full structural relaxations for all 6,832 infinite chains using density functional theory (DFT). To accurately account for electron correlation effects in the transition metals, we employed the DFT+U method, determining the Hubbard U and J values through a linear response approach. Subsequently, we calculated the formation enthalpies for all considered phases. In the third and final step, we assessed the thermodynamic stability of the candidate materials. By constructing thermodynamic stability phase diagrams based on the calculated formation enthalpies, we could identify the 1D chains that are stable against decomposition into competing phases.

To quantitatively identify the key factors governing thermodynamic stability, we employed a Random Forest (RF) classifier model[25]. The model was trained on a dataset derived from our high-throughput DFT calculations, using a set of 24 initial features—including chemical ratio and fundamental elemental properties—to predict a binary 'Stable' or 'Unstable' label for each material. The implementation of the model and its parameters, such as handling class imbalance with `class_weight='balanced'`, were based on the scikit-learn library[26]. To ensure statistical robustness, we evaluated the model using a stratified 5-fold cross-validation scheme[27] and repeated this entire procedure 50 times with different random seeds. The final feature importance scores were determined by averaging the Gini importance values, a standard metric in Random Forests<sup>[1]</sup>, across all trained models (5 folds  $\times$  50 repeats), providing a reliable measure of each feature's contribution to predicting stability.

## Acknowledgements

We gratefully acknowledge the financial support from the National Natural Science Foundation of China (Grants No. 92477205 and No. 52461160327), the National Key R&D Program of China (Grant No. 2023YFA1406500). Calculations were performed at the Physics Lab of High-Performance Computing (PLHPC) and the Public Computing Cloud (PCC) of Renmin University of China.

## References

- [1]. An, C., Zhang, Z., Wu, M., Wang, F., & Liu, Y. (2021). Recent advances in one-dimensional van der Waals heterostructures. *InfoMat*, 3(8), 839-860.
- [2]. Jain, A., Ong, S. P., Hautier, G., Chen, W., Richards, W. D., Dacek, S., ... & Persson, K. A. (2013). The Materials Project: A materials genome approach to accelerating materials innovation. *APL Materials*, 1(1), 011002.
- [3]. Šmejkal, L., Sinova, J., & Jungwirth, T. (2022). Beyond conventional ferromagnetism and antiferromagnetism: A review on spintronics with altermagnets. *Journal of Physics: Condensed Matter*, 34(41), 413001.
- [4]. Sander, D. (2004). The magnetic anisotropy and magnetostriction of epitaxial films and multilayers. *Journal of Physics: Condensed Matter*, 16(20), R603.
- [5]. Grüner, G. (1988). The dynamics of charge-density waves. *Reviews of Modern Physics*, 60(4), 1129-1181.
- [6]. Nadj-Perge, S., Drozdov, I. K., Li, J., Chen, H., Jeon, S., Seo, J., ... & Yazdani, A. (2014). Observation of Majorana fermions in ferromagnetic atomic chains on a superconductor. *Science*, 346(6208), 492-497.
- [7]. Geim, A. K., & Novoselov, K. S. (2007). The rise of graphene. *Nature Materials*, 6(3), 183-191.
- [8]. Gong, C., & Zhang, X. (2019). Two-dimensional magnetic crystals and van der Waals heterostructures. *Science*, 363(6428), eaav4450.
- [9]. Manzeli, S., Ovchinnikov, D., Pasquier, D., Yazyev, O. V., & Kis, A. (2017). 2D transition metal dichalcogenides. *Nature Reviews Materials*, 2(8), 17033.
- [10]. Liu, Y., Weiss, N. O., Duan, X., Cheng, H. C., Huang, Y., & Duan, X. (2016). Van der Waals heterostructures and devices. *Nature Reviews Materials*, 1(9), 16042.
- [11]. Mermin, N. D., & Wagner, H. (1966). Absence of ferromagnetism or antiferromagnetism in one- or two-dimensional isotropic Heisenberg models. *Physical Review Letters*, 17(22), 1133.
- [12]. Giamarchi, T. (2003). *Quantum Physics in One Dimension*. Oxford University Press.
- [13]. Blundell, S. (2001). *Magnetism in Condensed Matter*. Oxford University Press.
- [14]. Ising, E. (1925). Beitrag zur Theorie des Ferromagnetismus. *Zeitschrift für Physik*, 31(1), 253–258.
- [15]. Lu, S., Guo, D., Cheng, Z. et al. (2023). Controllable dimensionality conversion between 1D and 2D CrCl<sub>3</sub> magnetic nanostructures. *Nature Communications*, 14, 2465.
- [16]. Sun, B. W., Slassi, A., Zhang, Z., et al. (2021). Freestanding van der Waals single-atom-thick one-dimensional chains. *Nature*, 599(7885), 418–423.

- [17].Zhao, J., Sun, B. W., Zhang, Z., et al. (2022). Van der Waals gaps of carbon nanotubes as defined one-dimensional chemical reactors. *Nature*, 609(7927), 497–502.
- [18].Perdew, J. P., Burke, K., & Ernzerhof, M. (1996). Generalized Gradient Approximation Made Simple. *Physical Review Letters*, 77(18), 3865–3868.
- [19].Blöchl, P. E. (1994). Projector augmented-wave method. *Physical Review B*, 50(24), 17953–17979.
- [20].Kresse, G., & Hafner, J. (1993). Ab initio molecular dynamics for liquid metals. *Physical Review B*, 47(1), 558–561.
- [21].Kresse, G., & Furthmüller, J. (1996). Efficient iterative schemes for ab initio total-energy calculations using a plane-wave basis set. *Physical Review B*, 54(16), 11169–11186.
- [22].Grimme, S., Antony, J., Ehrlich, S., & Krieg, H. (2010). A consistent and accurate ab initio parametrization of density functional dispersion correction (DFT-D) for the 94 elements H-Pu. *The Journal of Chemical Physics*, 132(15), 154104.
- [23].Dudarev, S. L., Botton, G. A., Savrasov, S. Y., Humphreys, C. J., & Sutton, A. P. (1998). Electron-energy-loss spectra and the structural stability of nickel oxide: An LSDA+U study. *Physical Review B*, 57(3), 1505–1509.
- [24].Cococcioni, M., & de Gironcoli, S. (2005). Linear response approach to the calculation of the effective interaction parameters in the LDA+U method. *Physical Review B*, 71(3), 035105.
- [25].Breiman, L. (2001). Random Forests. *Machine Learning*, 45(1), 5–32.
- [26].Pedregosa, F., Varoquaux, G., Gramfort, A., et al. (2011). Scikit-learn: Machine Learning in Python. *Journal of Machine Learning Research*, 12, 2825–2830.
- [27].Kohavi, R. (1995). A Study of Cross-Validation and Bootstrap for Accuracy Estimation and Model Selection. In *Proceedings of the 14th International Joint Conference on Artificial Intelligence (IJCAI'95)*, Vol. 2, 1137–1143.